Catalysis Science & Technology

Accepted Manuscript

ROYAL SOCIETY OF CHEMISTRY

www.rsc.org/catalysis

Catalysis Science & Technology

ARTICLE

A one-step Cu/ZnO Quasi-Homogeneous Catalyst for DME Production from Syn-gas

Received 00th January 20xx,
Accepted 00th January 20xx

DOI: 10.1039/x0xx00000x

www.rsc.org/

A. García-Trenco,[a] E. White,[a] M.S. Shaffer[a]* and C. K. Williams[a]*

A simple one-pot synthetic method allows the preparation of hybrid catalysts, based on colloidal Cu/ZnO nanoparticles (NPs), used for the liquid phase synthesis of DME from syngas. The method obviates the high temperature calcinations and pre-reduction treatments typically associated with such catalysts. The hybrid catalysts are applied under typical industrially relevant conditions. The nature of the hybrid catalysts, the influence of the acid component, mass ratio between components, and Cu/Zn composition are assessed. The best catalysts comprise a colloidal mixture of Cu/ZnO NPs, as the methanol synthesis component, and γ-Al_2O_3, as the methanol dehydration component. These catalysts show high DME selectivity (65-70 %C). Interestingly, the activity (relative to Cu content) is up to three times higher than that for the reference hybrid catalyst based on the commercial Cu/ZnO/Al_2O_3 methanol synthesis catalyst. The hybrid catalysts are stable for at least 20 h time-on-stream, not showing any significant sintering of the Cu^0 phase. Post-catalysis,TEM/EDX shows that the hybrid catalysts consist of Cu^0 and ZnO NPs with an average size of 5-7 nm with γ-Al_2O_3 particles in close proximity.

1. Introduction

During the last decade, dimethyl ether (DME), a well-known intermediate for the production of valuable chemicals like light olefins or dimethyl sulphate, has received increasing attention as a synthetic substitute for conventional diesel due to its high cetane number and clean burning properties.[1,2] Traditionally, DME has been produced by a two-step process involving the synthesis of methanol from syn-gas, and the subsequent dehydration of methanol to DME. Nonetheless, a more economical route to produce DME based on a one-step process has lately been the subject of intensive research.[3-5] The main advantage of a direct route lies in the ability to remove the methanol synthesis equilibrium constraints and hence improve the thermodynamic driving force for DME production and potentially to allow a higher conversion of the reactants per-pass without the requirement of high pressures. Consequently, the route would reduce the need for costly gas recycle loops. Conventionally, the conversion of syn-gas to methanol is severely limited by the thermodynamic equilibria described by eqns. 1 and 2, however, the *in-situ* dehydration of methanol (3) is a favourable process and can be used to drive the equilibrium towards products. In addition, the water gas shift equilibrium (4) may remove the water, by-product, producing additional H_2 and CO_2, which are reactants for the methanol synthesis.

$$CO + 2H_2 \rightleftharpoons CH_3OH \quad (\Delta H°r=-90.8\ kJ/mol) \quad (1)$$
$$CO_2 + 3H_2 \rightleftharpoons CH_3OH + H_2O \quad (\Delta H°r=-49.5\ kJ/mol) \quad (2)$$
$$2CH_3OH \rightleftharpoons CH_3OCH_3 + H_2O \quad (\Delta H°r=-21.3\ kJ/mol) \quad (3)$$
$$H_2O + CO \rightleftharpoons H_2 + CO_2 \quad (\Delta H°r=-41.1\ kJ/mol) \quad (4)$$

Given that all the reactions are exothermic, the use of a liquid phase reactor may be beneficial, particularly compared to a conventional fixed bed reactor, as it facilitates heat removal and enables the reaction to be performed isothermally, in turn minimising catalyst deactivation commonly attributed to a poor temperature control.[6-10]

Hybrid catalytic systems comprising a heterogeneous Cu-based methanol synthesis catalyst and a solid acid as methanol dehydration catalyst are well suited for the direct DME synthesis process. Most often, the well-known heterogeneous Cu-ZnO-Al_2O_3 ternary methanol catalyst is combined with γ-Al_2O_3 or zeolites for methanol dehydration.[11-16] Typically, the calcined CuO-ZnO-Al_2O_3 precursor is mixed with the acid catalyst, and the resulting mixture reduced to give the active catalyst, containing metallic Cu.[13,15,17,18] However, such a methodology is not optimized for the two catalytic functions and thus, more targeted strategies have recently been reported.[19-23] Tsubaki et al. prepared core-shell hybrid catalysts, where the methanol synthesis is catalysed by a Cu-ZnO-Al_2O_3 core and it is dehydrated to DME by a zeolite shell.[19,20] Martínez et al. reported that the confinement of Cu-ZnO active sites in an SBA-15 ordered mesoporous silica, as the methanol synthesis function, mixed with HZSM-5, increased the catalyst stability by minimising the deactivation. This

[a] Department of Chemistry, Imperial College London, South Kensington, London, UK, SW7 2AZ; E-mail: m.shaffer@imperial.ac.uk, c.k.williams@imperial.ac.uk

† Footnotes relating to the title and/or authors should appear here.
Electronic Supplementary Information (ESI) available. See DOI: 10.1039/x0xx00000x

deactivation is attributed to both the sintering of copper, and to detrimental interactions between the Cu/ZnO and the acid function.[21,22] Wei et al. reported good activity and stability for hybrid catalysts comprising a Cu-based methanol synthesis catalyst supported on carbon nanotubes, mixed with γ-Al_2O_3 or HZSM-5.[23] More recently, Behrens et al. prepared hybrid catalysts by depositing pre-formed Cu and ZnO nanoparticles (NPs) onto the acid support (γ-Al_2O_3), which, after calcination, leads to immobilized CuO and ZnO NPs with a particle size of 7-16 nm.[24] Despite the fact that all of these catalytic systems show better performance than simple mixtures, there are some potential problems including complex preparation methodologies. Moreover, these hybrid catalysts have been tested in fixed-bed gas-phase configurations and so far, more sophisticated hybrid catalysts, able to function in the liquid phase for the synthesis of DME, remain unreported.

Over the last decade, mixtures of colloidal nanoparticles of Cu/ZnO, obtained from organometallic precursors, have emerged as interesting, high activity catalysts for liquid-phase, quasi-homogeneous, methanol synthesis; indeed, they show activities comparable to or slightly better than the reference Cu-ZnO-Al_2O_3 catalyst.[25-30] The improved activity is mainly attributed to the ability to finely disperse the Cu and ZnO phases, which leads to high surface areas and consequently to a high proportion of Cu/ZnO_x interface where the active sites for the methanol synthesis are widely proposed to be located.[31-34] Furthermore, colloidal catalysts offer a wide range of possibilities to 'tune' or control properties such as the particle size, solubility and functionality.[35,36] Previously, highly active colloidal catalysts for the hydrogenation of CO_2 to methanol were obtained by combining solutions of small nanoparticles of ZnO (3-5 nm) and Cu^0 (1-10 nm).[29] One drawback is that the system requires the separate preparation of the Cu^0 and ZnO nanoparticles. Recently, a simple, one-pot synthetic method to form Cu-ZnO colloidal catalysts was reported; this hybrid nanoparticle system, formed *in situ*, was found to be even more active for the hydrogenation of CO_2 to methanol.[30] The method consists of the reaction of diethyl zinc with a bis(carboxylate)copper (II) precursor, so as to form both Cu^0 and ZnO nanoparticles (ca. 5 nm) prior to or during the catalytic reaction. One interesting advantage of this method is that high temperature calcination and reduction steps which are usually required for methanol catalysts are avoided.

For the direct synthesis of DME from syn-gas, the development of a one-pot catalyst system, based on related colloidal nanoparticles would be desirable. Such a catalytic system should greatly facilitate the design and balance of the two catalytic functions. This work demonstrates the first example of colloidal catalysts for one-step DME synthesis and the exploration of the influence of the catalyst acid function, mass ratio, composition and nature on the formation of DME.

2. Experimental Section

2.1. Catalyst Preparation

2.1.1. Cu/ZnO Catalyst Precursors. Under an inert atmosphere, copper (II) bis(stearate),[37] synthesised according to the reported method,[38] and diethyl zinc (Sigma Aldrich) were mixed in dry toluene (distilled from sodium and degassed by performing at least three free-pump thaw cycles), at room temperature and using a total metal (Cu+Zn) concentration of 0.12 M. The resulting pre-catalyst colloid, denoted as Cu/Zn@st, was stirred for 1 h before being transferred to the reactor.

The commercial precursor to the methanol synthesis catalyst, a ternary CuO-ZnO-Al_2O_3 (abbreviated CZA) material, was obtained from Alfa Aesar (45776, mass composition CuO: 63.5%, ZnO; 25.1%, Al_2O_3; 10.1%, MgO; 1.3%) and ground from pellet to a fine powder using a pestle and mortar.

2.1.2. Dehydration catalysts. γ-Al_2O_3 was obtained commercially from Alfa Aesar (γ-Al_2O_3 nanopowders 44757) and is labelled as γAl. The starting NH_4-ZSM-5 zeolite (Alfa Aesar 45877), with a Si/Al nominal atomic ratio of 11.5, was converted to its H-form by calcination at 500 °C for 3 h (ramp 3 °C/min) under a flow of air, giving the sample HZ. Aliquots of this NH_4-ZSM-5 sample were Na-modified by incipient wetness impregnation, in order to attain Na/Al atomic ratios of 0.3 and 0.6. In detail, Na was incorporated using an aqueous solution of $NaNO_3$ (≥99%, Aldrich), followed by drying at 100 °C, for 20 h and calcination at 500 °C for 3 h (ramp 3 °C /min) in flowing air. The resulting materials were labelled as 0.3NaHZ (Na/Al of 0.3) and 0.6NaHZ (Na/Al of 0.6).

2.2. Characterization Techniques

The chemical compositions of the ZSM-5 samples were determined by Inductively Coupled Plasma-Optical Emission Spectroscopy (ICP-OES) in a Optima 3300 DV Perkin Elmer equipment. The solid samples were digested by alkaline fusion using lithium tetraborate and potassium iodide in a 10 wt% HNO_3 solution. Elemental analysis (EA) was carried out using a Carlo Erba Flash 2000 Elemental Analyser. Infrared (IR) spectroscopy was performed in a Perkin-Elmer Spectrum 100 Fourier Transform IR spectrometer with an Attenuated Total Reflection (ATR) accessory.

The acid strength distribution in the samples was determined by NH_3-TPD in a Micromeritics Autochem II 2920 coupled with a thermal conductivity detector (TCD). The samples (ca. 300 mg) were initially pre-treated at 450 °C, for 30 min under He, cooled to 150 °C and then saturated by flowing a mixture 5 vol% NH_3/He for 60 min. Afterwards, the residual NH_3 was completely purged from the system using a flow of He and finally, the chemisorbed ammonia was desorbed by heating from 150 °C to 700 °C, at a heating rate of 10 °C/min, under a flow of He gas (25 mL/min).

Powder X-ray diffraction (XRD) was performed using an X'Pert Pro MPD diffractometer (PANalytical B. V) operating at 40 kV and 40 mA, using nickel-filtered Cu Kα radiation (λ= 0.1542 nm). The average crystallite sizes of the Cu^0 and ZnO phases for the hybrid catalysts were determined by applying Scherrer's equation to the

most intense and non-overlapped reflections at 50.4° (200) and 56.7° (110), respectively. The preparation and analysis of the post-catalysis mixtures for XRD characterisation was performed using typical air-sensitive techniques. As such, the samples were withdrawn from the reactor, under a flow of nitrogen, washed with dry hexane, and subsequently dried under vacuum. Finally, the resulting solid powders were transferred to the sample holder of the diffractometer and the data collected.

TEM samples were prepared by drop-casting a toluene solution onto a 300 mesh Au holey carbon grid with an ultrathin 3 nm carbon film (Agar Scientific). ADF-STEM and EDX mapping were performed with a JEOL JEM 2100F scanning transmission electron microscope operated at 200 kV, and equipped with an Oxford X-Max 80 SDD EDX detector. HR-TEM images were obtained with an aberration corrected FEI Titan operated at 300 kV. For HR-TEM imaging, samples were loaded into a Gatan Environmental Holder, under a nitrogen atmosphere, preventing any atmospheric exposure that might lead to inadvertent oxidation of the Cu nanoparticles. The average sizes for the NPs were determined using ADF STEM by measuring more than 150 NPs for each sample.

2.3. Catalytic Experiments

The syn-gas-to-DME experiments were performed in a 300 mL autoclave reactor (Parr) which was mechanically stirred at 1500 r.p.m and with vertical baffles to ensure homogeneous mixing of the liquid and gas phase. Squalane was used as the reaction solvent as it exhibits a high boiling point and good gas solubility of the feed gases; it has already been reported as an excellent solvent for the liquid phase methanol synthesis process and is widely used.[39]

In a typical procedure, the reactor was filled with squalane (100 mL) and then stirred at room temperature, under a flow of N_2 (400 mL/min), for 30 min to de-gas the solvent. The pre-catalyst colloid (40 mL) was added, the reactor was heated to 260 °C and then pressurized to 5.0 MPa using a gas mixture comprising 95 vol% syn-gas (70% H_2/24% CO/6% CO_2) and 5 vol% Ar (used as internal standard for GC analysis). The reactor was kept under these conditions, flowing 125 mL/min of the gas mixture, for 1 h, so as to hydrolyse the zinc ethyl compounds present in the pre-catalyst colloid to ZnO.[30] Next, the reactor was cooled to 100 °C, evacuated, and the required amount of the methanol dehydration component was added (suspended in 10 mL of degassed squalane), under a N_2 flow. The syn-gas-to-DME runs were performed at 260 °C, 5.0 MPa and space velocity of 7.4 $L_{syngas}/g_{CuZn}/h$ using a concentration of the methanol synthesis catalyst in the reactor of 2.1 g_{CuZn}/L. Control experiments indicated that the overall reaction rate was not controlled by mass transport phenomena, under the conditions studied. The resulting hybrid catalysts were labelled as CuZnO@st/*x*, where *x* stands for the methanol dehydration component used.

The reference catalyst, a mixture of Cu-ZnO-Al_2O_3/γ-Al_2O_3 (abbreviated CZA/γAl), was prepared by physically mixing the fine powders of the CZA and γ-Al_2O_3 materials (CuZnO/γ-Al_2O_3 mass ratio 1:2) until a homogeneous mixture was observed. Afterwards, the required volume of squalane was added to the reactor so as to maintain a concentration of 2.1 g_{CuZn}/L and then degassed using a flow of N_2. Before conducting the experiment, the reference catalyst was activated using a diluted H_2 stream (5 vol% H_2/N_2) at 0.45 MPa and 240 °C (ramp 2 °C/min) for 4 h, according to a standard activation protocol for the ternary Cu-ZnO-Al_2O_3 methanol synthesis catalysts in slurry reactors.[40] Finally, the catalytic run was performed under the same reaction conditions described above.

The reaction products and unreacted materials were monitored by an online Gas Chromatograph (Bruker 450-GC), equipped with a TCD, for the quantification of CO, CO_2 and Ar, and a FID, for the quantification of the oxygenates (MeOH, DME) and hydrocarbons. To avoid any product condensation during the experiments, the lines from the reactor to the injection port of the GC were heated to 180 °C. The catalytic results are presented once the pseudo-steady state and maximum activity were attained (~5 h TOS). Product yields and selectivities are given on a carbon basis and were determined considering the amount of CO_2 present in the syn-gas feed. Carbon mass balances for the runs were 100±2% and the error for measurements determined by repeated runs was ±2%.

3. Results and Discussion

3.1. Formation of the colloidal Cu/ZnO methanol synthesis component.

Mixing copper(II) bis(stearate) (Table S1 and Fig. S1),[41] and diethyl zinc, under the appropriate conditions in toluene, leads to the formation of a pre-catalyst colloid consisting of Cu^0 nanoparticles and a mixture of diethyl zinc and a heteroleptic alkyl zinc carboxylate complex species.[30,42-44] It is proposed that ligand exchange occurs between the copper and zinc complexes leading to the formation of copper-alkyl species that rapidly decomposes to give metallic copper NPS.[30,45] The formation of well-defined metallic Cu NPs with an average size of 5 nm, regardless of the Cu/Zn composition used, was confirmed by HR-TEM (Fig 1, Table S2). Characteristic (111) lattice spacings of crystalline metallic copper are clearly visible (Fig. 1c). The individualised nature of the NPs indicates that they are effectively surface modified and stabilised likely by stearate. The pre-catalyst colloid solution was added to the reactor containing the reaction solvent (squalane) and exposed to

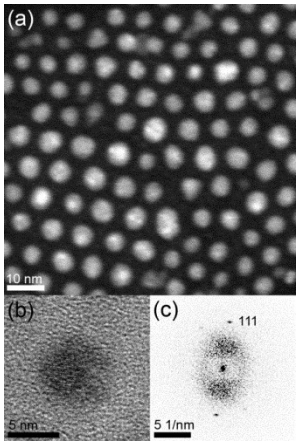

Fig. 1. Representative images of the Cu^0 nanoparticles stabilised by stearate in the pre-catalyst colloid a) ADF-STEM image, b) HR-TEM image and c) Fourier transform of the HR-TEM image.

syn-gas at 260 °C and 5.0 MPa. The water produced in the methanol synthesis enables the hydrolysis of the $ZnEt_2$ groups leading to the *in-situ* formation of ca. 5 nm ZnO nanoparticles (*vide infra*).[30] The hydrolysis of the zinc-ethyl moieties released mostly ethane, as detected by the on-line GC instrument during the first hour of reaction. The combination of the Cu^0 and ZnO nanoparticles, each stabilized by the stearate ligand (derived from the copper precursor), comprise the active colloidal catalyst used with the methanol synthesis component in the hybrid catalyst employed. A detailed characterisation of the pre-catalyst colloid and the resulting active catalyst are described in the previous work.[30]

3.2. The Methanol Dehydration Components

Typically, γ-Al_2O_3 or zeolite ZSM-5 are the acid catalyst components used for the methanol dehydration function.[11,13-16] Generally, zeolites have been observed to be more active than γ-Al_2O_3 due to their Brønsted acidity and greater hydrophobicity which prevents the adsorption of water.[12,46] It is also proposed that the strongest acidic sites on zeolites can promote the subsequent dehydration of DME to hydrocarbons, leading to reduced DME selectivity.[12,13] In order to overcome this limitation, the strongest Brønsted acid sites are commonly neutralized by means of a partial ionic exchange with Na^+, Mg^{2+} or Al^{3+}.[10,13,14,46] Thus, γ-Al_2O_3, HZSM-5 and Na-modified ZSM-5 samples, with different Na contents, were assessed in order to establish the most suitable methanol dehydration component.

The chemical composition of the zeolite materials was studied using ICP-OES and the corresponding results are shown in Table S3. As expected, the overall Si/Al atomic ratio agrees well with the nominal ratio given by the commercial supplier (Si/Al= 11.5). Furthermore, the Na/Al ratio for the NaHZ samples corresponds exactly to the value expected from the concentration of the Na precursor in the impregnating solution.

The changes in the acid strength distribution of the ZSM-5 samples, both before and after modification, were addressed with NH_3-TPD characterization. As shown in Fig. 2, the zeolite ZSM-5 in its protonated form (HZ) exhibits two main desorption peaks at 237 and 431 °C, attributed to the weak and strong acid sites, respectively. Upon increasing the Na content, for the NaHZ samples, the signal attributed to the strong acid sites decreases and the signal attributed to the weak sites is enhanced. This change suggests that the Na^+ cations are preferentially exchanged with the strongest Brønsted acid sites of the zeolite. In fact, most of the strong acid sites are neutralised with the Na/Al ratio of 0.6 (0.6NaHZ). The increase in the amount of weak acid sites could be attributed to the formation of Lewis-acidic Na^+ sites in the exchange positions of the zeolite. Unlike the NH_3-TPD profiles obtained for the ZSM-5 materials, γ-Al_2O_3 (γAl) displays only the presence of weak acid sites, with the main desorption peak observed at T_{max}= 261 °C together with a shoulder at lower temperatures (T_{max}= 205 °C). Overall the γAl has a much lower overall concentration of acid sites than the zeolites (Table S3).

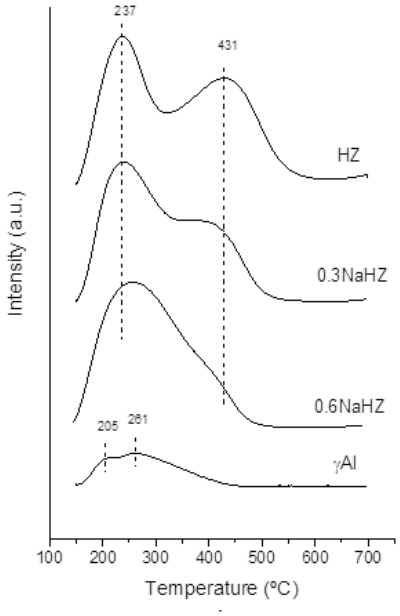

Fig. 2. NH_3-TPD profiles for the HZ, NaHZ and γAl acid samples.

3.3. The hybrid catalysts

The hybrid catalysts were prepared by mixing the pre-formed CuZnO colloidal catalysts, containing equimolar quantities of Cu and ZnO, with the acid catalysts, γAl, HZ, NaHZ or NaZ. A control CuZnO@st catalyst, without an acidic component, leads to a 32% conversion of CO and is highly selective to methanol (96%) (Fig. 3, Table S4). Despite previous pioneering work using similar CuZnO colloids as model catalysts for the methanol synthesis,[25,26] there are no previous reports of any such high conversions of the reactants, which would be required for any industrial application.[6] For the hybrid catalysts, an increase in the CO conversion, to values higher than 50%, was observed in all cases. Such results are encouraging and clearly demonstrate the potential for such synergic hybrid catalysis to overcome the methanol synthesis equilibrium limitations. Hence, it can also be inferred that the CO conversion when using only the CuZnO@st catalyst is limited by thermodynamic constraints.

As well as leading to high CO conversions (53-59%), Fig. 3 shows that all the hybrid catalysts, regardless the acid component, efficiently dehydrate the methanol present in the medium, as shown by the low MeOH selectivity values (<4%). However, the selectivity to DME and hydrocarbons (HC), depends on the strength of the acidic component. The use of γ-Al_2O_3 leads to high DME selectivity (65%), with negligible HC production (0.1% selectivity). In contrast, the use of zeolites produces greater amounts of HC, mostly in the range C_1-C_5.

The parallel increase in the quantities of hydrocarbon and CO_2 produced can be explained by the dehydration of DME to hydrocarbons leading to the formation of water, which is rapidly converted to CO_2, through the water gas shift reaction, a process known to be catalysed by Cu/ZnO surfaces.[13] The production of hydrocarbons is at the expense of the DME selectivity, without

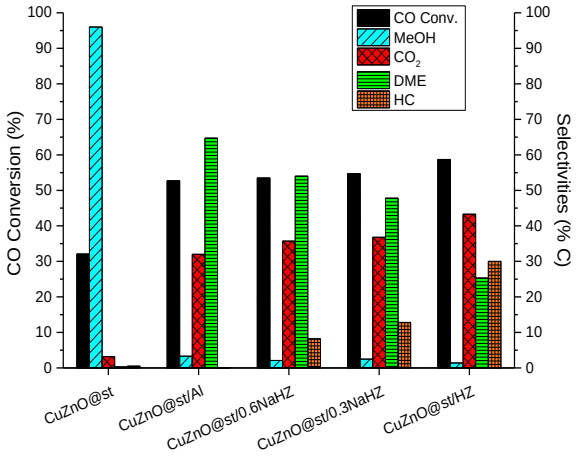

Fig. 3. CO conversions and selectivities for CuZnO@st/γAl hybrid catalysts prepared with a CuZnO/x mass ratio of 1/1. Reaction conditions: 260 °C, 5.0 MPa, GHSV= 7.4 $L_{syn\text{-}gas}/g_{CuZn}$/h and syn-gas composition 70%H_2/24%CO/6%CO_2.

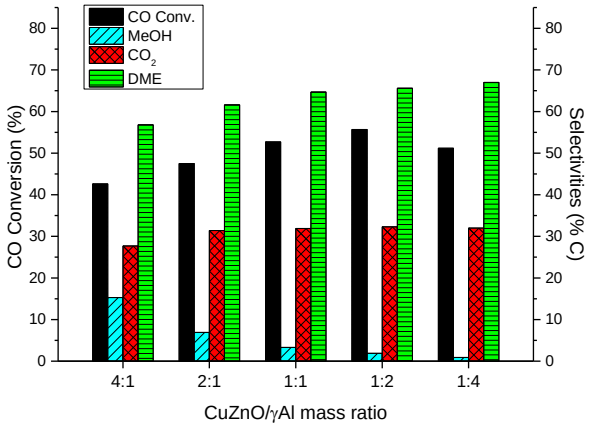

Fig. 4. Direct synthesis of DME runs for the CuZnO@st/γAl hybrid catalysts by changing the CuZnO/γ-Al_2O_3 mass ratio. Reaction conditions: 260 °C, 5.0 MPa, GHSV= 7.4 L_{syngas}/g_{CuZn}/h and syn-gas composition 70%H_2/24%CO/6%CO_2.

significantly increasing overall CO conversion. Increasing the Na content in the zeolites, and reducing the concentration of strong acidic functional groups, leads to a significant reduction in HC by-product formation and thus, an increase in DME selectivity. The use of γ-Al_2O_3, which has no strong acid sites, results in the highest DME selectivity.

3.4. Influence of the Cu-ZnO@st/γ-Al_2O_3 ratio

Since the catalysts combining Cu-ZnO colloids with γ-Al_2O_3 show good activities and the best selectivities to DME, they were studied further; specifically, the mass ratio of γ-Al_2O_3 added to the colloidal CuZnO component was adjusted. As shown in Figure 4 (Table S5), the initial increase in γ-Al_2O_3 concentration reduces the methanol selectivity in favour of DME, which is expected due to the more efficient dehydration of methanol in the medium. Once a Cu-ZnO/γ-Al_2O_3 mass ratio of 1:1 is attained, any further increase in the γ-Al_2O_3 content only slightly affects the corresponding selectivities. It is also notable that hydrocarbons are not produced, even using the highest γ-Al_2O_3 content (highest concentration of acidic sites).

The addition of γ-Al_2O_3 systematically increased the total conversion of CO, as the DME synthesis rate is controlled by the methanol dehydration step.[13,14] However, the conversion reached a maximum (56%) at the Cu-ZnO/γ-Al_2O_3 mass ratio of 1:2. Once there is sufficient γ-Al_2O_3 to dehydrate essentially all the methanol produced, further additions of γ-Al_2O_3 lead to an excess of acid sites and should have little effect. Nevertheless, this further addition produces a modest drop in overall CO conversion. Although an explanation for this loss in CO conversion at the highest γ-Al_2O_3 is still not clear, it may be that the large alumina surface area absorbs some components from the Cu/ZnO surface, or migrates to the Cu/ZnO component blocking active methanol synthesis sites.[47,48] Overall, the best conditions are a Cu-ZnO/γ-Al_2O_3 mass ratio of 1:2, which results in the highest CO conversion and DME yield (37 %, Table S5).

3.5. Influence of the Cu/Zn ratio.

The colloidal approach also allows the Cu/Zn catalyst composition to be adjusted, simply and across a broad range, by modifying the proportions of organometallic precursors used to prepare the colloid nanoparticles. In contrast with conventional catalyst (Cu/ZnO/Al_2O_3) synthesis methods, this flexibility allows both the rapid and easy investigation of the optimum relative quantities of Cu and ZnO in the methanol synthesis component. These quantities were therefore investigated whilst maintaining the overall CuZnO/γAl mass ratio of 1:2. As explored in the previous section, at this γAl concentration, any MeOH produced is immediately converted to DME and under these conditions the overall process rate is governed by the methanol synthesis rate on the CuZnO@st catalyst.[13,14]

As shown in Fig. S2 (Table S6), all the catalysts exhibited similar selectivities to the main reaction products (1-3% MeOH, 66-70% DME, and 28-32% CO_2) regardless of the methanol synthesis catalyst composition. On the other hand, there is a strong correlation between the conversion of CO and the Cu/ZnO ratio, which confirms that the process is controlled by the methanol synthesis component. The optimum CO conversion (56%) is obtained for a catalyst comprising equimolar quantities of Cu and Zn (Zn/(Cu+Zn) molar ratio of 0.5). There are several hypotheses in the literature to rationalize such experimental observations: some authors discuss the active site comprising a metallic Cu-Zn alloy,[49] others by key Cu facets being stabilized by ZnO,[50,51] and yet another hypothesis is that there are Cu^0 steps decorated with Zn atoms[52] or oxygen vacancies in the ZnO generated by metallic Cu.[34] Regardless of the precise nature of the active site or sites, it is now widely accepted that a Cu/ZnO interface is required to form the active site and thus, strategies to maximise the interface are important to improve activity.[34,53] The extent of Cu interacting with ZnO can be estimated by comparing the activity per mass of Cu for the catalysts. Using such an approach for the hybrid catalysts, Fig. 5

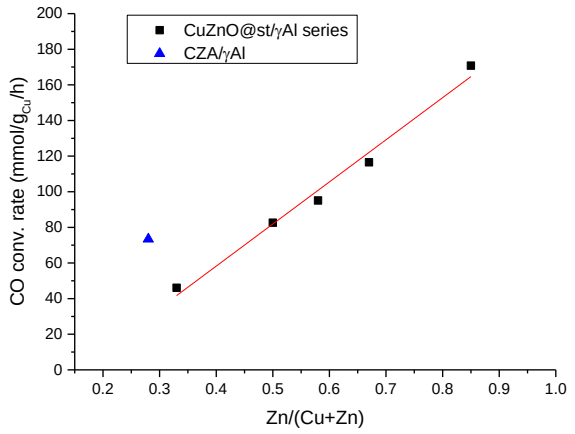

Fig. 5. CO conversion rate (per mass of copper) as a function of Zn content for the CuZnO@st/γAl and the reference CZA/γAl hybrid catalysts.

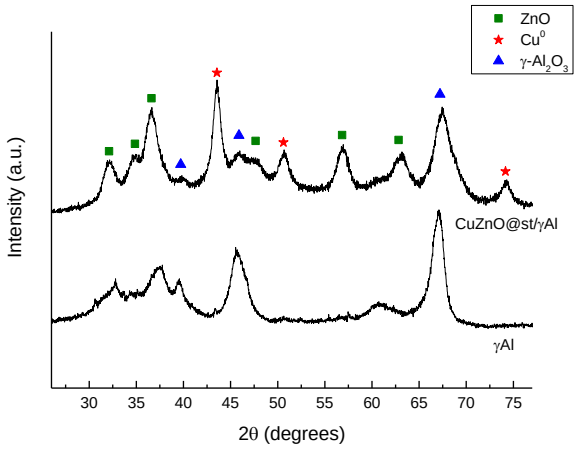

Fig. 6. XRD pattern for the post-catalysis sample CuZnO@st/γAl with a Cu/Zn ratio (CuZnO/γ-Al_2O_3 mass ratio of 1/2) and γAl acid material is included as reference

shows a linear correlation between the activity per mass of Cu and the Zn/(Cu+Zn) ratio. Essentially, at higher copper dilution with ZnO, proportionally more copper is able to form an active interface with ZnO in the composition range studied, which explains the observed increase in activity.

For comparative purposes, a hybrid reference catalyst system was evaluated based on the commercial Cu-ZnO-Al_2O_3 methanol synthesis catalyst and γ-Al_2O_3 (CZA/γAl). Under the same reaction conditions, the selectivity values for the main reaction products are in the range of those obtained for the colloidal-based hybrid catalysts (Fig. S2, Table S6). The CO conversion is ~30% higher than that achieved for the optimum CuZnO@st/γAl catalyst, in terms of Cu+Zn mass. When the activity is considered on a Cu basis, as just discussed, the colloidal-based hybrid catalysts exhibit up to three-times greater activity compared to the reference CZA/γAl (Fig. 5). This increased activity is explained by the colloidal particles having a significantly higher Cu metallic surface available for the ZnO interaction, enabled by the ability to adjust the Cu/Zn composition.

3.6. Nature of the CuZnO@st/γAl hybrid catalysts.

The nature of the optimum colloidal-based hybrid catalyst (CuZnO@st/γAl with a Cu/Zn ratio of 1 and CuZnO/γ-Al_2O_3 mass ratio of 1/2) was studied by analysing a post-catalysis sample, after exposure to the reaction conditions for 20 h. Although the detailed stability and deactivation mechanisms are beyond the scope of the current work, it is worth noting that near constant activity and selectivity values were observed for at least 20 hours (Fig. S3 and Fig. S4). These results are promising considering that a substantial loss in activity over short time scales is one of the main problems encountered for other bifunctional catalysts for DME synthesis.[18,21,54]

The XRD pattern for the CuZnO@st/γAl shows reflections related to Cu^0 (ICDD 001-1241), ZnO (ICDD 075-0576) and γ-Al_2O_3 (ICDD 046-1131) phases (Fig. 6). No diffraction features attributed to other phases, such as Cu_2O or CuO, were detected, indicating this that the majority of the copper components remain metallic during the reaction. The XRD also confirms the formation of ZnO NPs from the *in-situ* hydrolysis of the organometallic precursor $ZnEt_2$.[30] The broad reflections are attributed to the presence of small crystallites: the average crystallite sizes, estimated from Cu^0 (200) and ZnO (110) were 7.5 and 6.5 nm, respectively.

Detailed examination of the optimised CuZnO@st component of the hybrid catalyst, using HR-TEM images, revealed the presence of Cu^0 and ZnO NPs in direct contact (Fig. 7). As discussed in the previous section, the active sites for the methanol synthesis are widely considered to be located at the Cu^0/ZnO interface, although the exact nature of the active site remains the subject of debate.[49-53]. ADF-STEM images (example in Fig. 8) for the optimum catalyst present intimate mixed agglomerates of equiaxed Cu and Zn-containing NPs along with larger γ-Al_2O_3 particles. The average distance between the NPs and γ-Al_2O_3 particles, performing hundreds of measures onto the EDX maps from the ADF-STEM images, is 20 nm, being the maximum distance obtained smaller than 100 nm. These data confirm that both catalytic components are in very close proximity in the reaction medium, and hence explain their effectiveness as a hybrid system. Whilst the exact

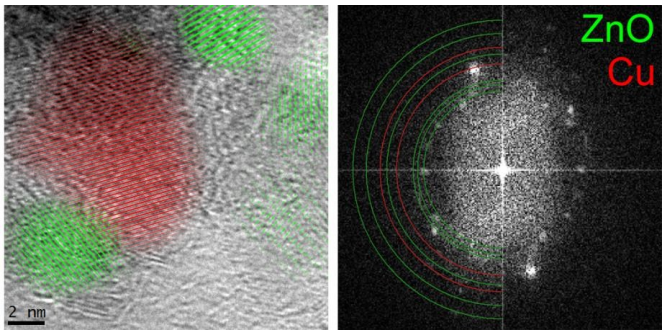

Fig. 7. Representative HR-TEM image (left) of the CuZnO@st component in the hybrid catalysts; Cu^0 and ZnO NPs are red and green, respectively. Peaks in the Fourier ransform (right) correspond to lattice spacings in the HR-TEM image. In the left hand of the Fourier transform, ring indicate the lattice spacings of wurtzite ZnO and Cu^0, which uniquely identify the NPS.

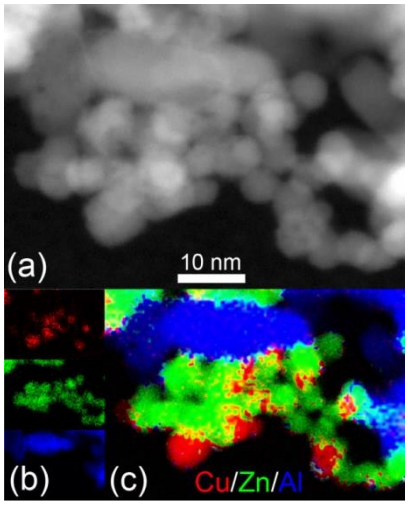

Fig. 8. a) Representative ADF-STEM image of the post-catalysis sample CuZnO@st/γAl with a Cu/Zn ratio of 1 and CuZnO/γ-Al_2O_3 mass ratio of 1/2. b) Cu (red), Zn (green) and Al (blue) EDX maps. c) overlay of b and a showing the location of Cu, Zn and Al-containing NPs.

minimum separation required to produce this characteristic synergy is unknown, and is likely to depend on mass transport rates under specific reaction conditions, it is known that an intimate mixture is advantageous for the direct synthesis of DME.[11,55]

The average particle sizes estimated for the Cu and Zn-containing NPs were 6.0 (±2.0) and 6.6 (±1.0) nm, in good agreement with the values obtained by XRD characterisation. The average size of the Cu^0 NPs for the corresponding pre-catalyst colloid was 4.7 (±1.7) nm (Table S2), hinting at some ripening during reaction, but no firm conclusion can be drawn given that the change is less than the statistical errors. Nevertheless, it is clear that any particle growth is modest; the low sintering rate of the catalyst particles can be tentatively attributed to the presence of the stearate ligand stabilising the nanoparticles. In support of this hypothesis, the immobilisation of colloidal Cu/ZnO NPs onto γ-Al_2O_3 by means of air calcination, which removes the organic ligand, has been recently reported to result in a significant degree of particle sintering, particularly for the Cu^0 NPs, after exposing the catalyst to the direct synthesis of DME for less than 3 h time-on-stream.[24] In fact, in this previous study, an increase in the average Cu^0 crystallite size from 7 nm to 16 nm was obtained even in the best case.[24] In order to prove this hypothesis, a control experiment was performed using copper (II) bis(acetate), to prepare the colloidal Cu/ZnO NPs; the much shorter ligand is not expected to provide steric stabilisation to prevent the ripening of the Cu^0 and ZnO NPs. XRD characterisation of the acetate-derived pre-catalyst colloid showed small Cu^0 crystallites with an average size of 2.7 nm; however, the post-catalysis sample revealed the presence of larger Cu^0 and ZnO crystallites, 21.6 and 25.9 nm, respectively (Fig. S5). These results are consistent with post-catalysis ADF-STEM images showing NPs sized 20-30 nm (Fig. S6). Therefore, the low ripening rate of the Cu^0 (and probably ZnO NPs), during the reaction, can be attributed to the presence of the stearate ligand in the reaction medium. Copper sintering is one of the typical deactivation modes reported for catalysts employed in the methanol synthesis and direct DME synthesis[21,56] and thus, it is inferred that the use of the colloidal CuZnO materials may represent a promising means to alleviate or slow this deactivation mode.

4. Conclusions

A simple methodology to prepare hybrid catalysts for the liquid phase production of DME from syn-gas is described. The catalysts have two parts: 1) a colloidal Cu/ZnO methanol synthesis catalyst and 2) an acid component for the methanol dehydration. The method may be attractive as it combines good performance metrics, including good activity and selectivity, with straightforward catalyst preparation. In particular, it avoids high temperature calcinations and the need for any pre-reduction treatments, typically associated with previous reports of catalysts for methanol or DME synthesis. The hybrid catalysts were applied in the direct synthesis of DME, in the liquid phase and under typical industrially-relevant conditions, and the impact of variables such as the component acidity, the catalyst composition, the Cu/Zn ratio, and the nature of the hybrid catalysts have been correlated to the performance of the catalyst, as assessed by activity and selectivity measures. Using catalysts comprising a CuZnO/γ-Al_2O_3 mass ratio of 1/2 shows the best performance, providing sufficient activity to dehydrate essentially all the methanol produced, without interfering with the methanol synthesis component; in addition, for DME production, it is necessary to avoid dehydration catalysts showing high proportions of strongly acidic sites. One benefit of the colloidal methanol synthesis catalysts is the facility to tune the Cu/ZnO ratio; this approach has led to an optimum activity which is up to three-fold higher than that for reference Cu-ZnO-Al_2O_3/γ-Al_2O_3 hybrid catalyst, based on the loading of Cu.

The optimum hybrid catalyst exhibited good stability and DME selectivity under reaction conditions (for at least 20 h). Characterization of a post-catalysis sample revealed that there are small Cu and ZnO nanoparticles (sized 5-7 nm) in close proximity to the γ-Al_2O_3. Moreover, a low degree of Cu^0 sintering was observed after the catalytic runs, a finding which is potentially attractive in terms of preparation of hybrid catalysts showing enhanced stabilities as well as activities.

Thus, the use of the hybrid catalysts enables the direct synthesis of DME, in the liquid phase, and leads to excellent performance, under industrially-relevant conditions. The study demonstrates the potential for such systems and indicates that future further development, including investigation of other ancillary ligands, metals and process conditions is warranted.

Acknowledgements

At Imperial College London, the EPSRC are acknowledged for funding (EP/H046380, EP/K035274/1).

Notes and references

1. T.A. Semelsberger, R.L. Borup and H.L. Greene, *J. Power Sources, 2006,* **156**, 497-511.
2. N. Inoue and Y. Ohno, *Petrotech,* 2001, **24**, 319-322.
3. J. Topp-Jorgensen, *US Patent 4,536,485,* 1985.
4. J.B. Hansen, F.H. Joensen and H.F.A. Topsoe, *US Patent 5,189,203,* 1993.
5. T. Shikada, Y. Ohno, T. Ogawa, M. Ono, M. Mizuguchi, K. Tomura and K. Fujimoto, *Stud. Surf. Sci. Catal.*, 1998, **119**, 515-520.
6. S. Lee and A. Sardesai, *Top. Catal.*, 2005, **32**, 197-207.

7. T. Ogawa, N. Inoue, T. Shikada and Y. Ohno, *J. Nat. Gas Chem.,* 2003, **12**, 219–227
8. G. Moradi, J. Ahmadpour and F. Yaripour, *Energy Fuels,* 2008, **22,** 3587-3593.
9. Y. Tan, H. Xie, H. Cui, Y. Han and B. Zhang, *Catal. Today,* 2005, **104**, 25-29.
10. N. Khandan, M. Kazemeini and M. Aghaziarati, *Catal. Lett*., 2009, **129**, 111-118.
11. Q. Ge, Y. Huang, F. Qiu and S. Li, *Appl. Catal. A,* 1998, **167**, 23-30.
12. T. Takeguchi, K. Yanagisawa, T. Inui and M. Inoue, *Appl. Catal*. *A*, 2000, **192**, 201-209.
13. D. Mao, W. Yang, J. Xia, B. Zhang, Q. Song and Q. Chen, *J. Catal*., 2005, **230**, 140-149.
14. A. García-Trenco and A. Martínez, *Appl. Catal. A,* 2012, **411-412**, 170-179.
15. A. García-Trenco, S. Valencia and A. Martínez, *Appl. Catal. A,* 2013, **468**, 102-111.
16. J.W. Bae, S.-H. Kang, Y.-J. Lee and K.-W Jun, *J. Ind. Eng. Chem*., 2009, **15**, 566-572.
17. J.-H. Kim, M.J. Park, S.J. Kim, O.-S. Joo and K.-D. Jung, *Appl. Catal. A,* 2004, **264**, 235-240.
18. J. Ereña, J. Vicente, A.T. Aguayo, M. Olazar, J. Bilbao and A.G. Gayubo, *Appl. Catal. B,* 2013*,* **142-143**, 315-322.
19. G. Yang, N. Tsubaki, J. Shamoto, Y. Yoneyama and Y. Zhang, *J. Am. Chem. Soc*., 2010, **132**, 8129-8136.
20. G. Yang, M. Thangkan, T. Vitidsant, Y. Yoneyama, Y. Tan and N. Tsubaki, *Catal. Today,* 2011*,* **171**, 229-235.
21. A. García-Trenco and A. Martínez, *Appl. Catal. A,* 2015*,* **493**, 40-49.
22. A. García-Trenco and A. Martínez, *Catal. Today,* 2013*,* **215**, 152-161.
23. Q. Zhang, Y.-Z. Zuo, M.-H. Han, J.-F. Wang, Y. Jin and F. Wei, *Catal. Today,* 2010*,* **150**, 55-60.
24. M. Gentzen, W. Habicht, D.E. Doronkin, J.-D. Grunwaldt, J. Sauer and S. Behrens, *Catal. Sci. Technol.,* DOI: 10.1039/C5CY01043H.
25. M.K. Schröter, L. Khodeir, M.W.E. van den Berg, T. Hikov, M. Cokoja, S. Miao, W. Grünert, M. Muhler and R.A. Fischer, *Chem. Commun*., 2006, 2498-2500
26. S. Chimpf, A. Rittermeier, X. Zhang, Z.-A. Li, M. Spasova, M.W.E. van den Berg, M. Farle, Y. Wang, R.A. Fischer and M. Muhler, *Chem. Cat. Chem*., 2010, **2**, 214-222.
27. A. Rittermeier, S. Miao, M.K. Schröter, X.Zhang, M.W.E van den Berg, S. Kundu, Y. Wang, S. Schimpf, E. Löffler, R.A. Fischer and M. Muhler, *Phys. Chem. Chem. Phys*., 2009, **11**, 8358-8366.
28. M.A. Sliem, S. Turner, D. Heeskens, S.B. Kalidindi, G.V. Tendeloo, M. Muhler and R.A. Fischer, *Phys. Chem. Chem. Phys*., 2012, **14**, 8170-8178.
29. N.J. Brown, J. Weiner, K. Hellgardt, M.S.P. Shaffer and C.K. Williams, *Chem. Commun*., 2013, **49**, 11074-11076.
30. N.J. Brown, A. García-Trenco, J. Weiner, E.R. White, M. Allinson, Y. Chen, P.P. Wells, E.K. Gibson, K. Hellgardt, M.S.P. Shaffer and C.K. Williams, *ACS Catal*., 2015, **5**, 2895-2902.
31. J. Nakamura, I. Nakamura, T. Uchijima, Y. Kanai, T. Watanabe, N. Saito and T. Fujitani, *J. Catal*., 1996, **160**, 65-75.
32. M.W.E. van den Berg, S. Polartz, O.P. Tkachenko, K. Kahler, M. Muhler and W. Grünert, *Catal. Lett*., 2009, **128**, 49-56.
33. E.K. Poels and D.S. Brands, *Appl. Catal*. *A,* 2000, **191**, 83-96.
34. A. Le Valant, C. Comminges, C. Tisseraud, C. Canaff, L. Pinard and Y. Pouilloux, *J. Catal.,* 2015*,* **324**, 41-49.
35. J. Grunes, J. Zhu and G.A. Somorjai, *Chem. Commun*., 2003, 2257-2260.
36. D. Astruc, F. Lu and J.R. Arazanes, *Angew. Chem. Int. Ed*., 2005, **44**, 7852-7872.
37. A.M. Godquin, J.C. Marchon, D. Guillon and A. Skoulios, *J. Phys. Lett*., 1984, **45**, L681-L684.
38. Y.F. Hsu, C.P. Cheng, *J. Mol. Catal. A*, 1998, **136**, 1-11.
39. G.P. van der Laan, A. A.C.M. Beenackers, B. Ding and J.C. Strikwerda, *Catal. Today,* 1999*,* **48**, 93-100.
40. A. Sawant, M.K. Ko, V. Parameswaran, S. Lee and C.J. Kulik, *J. Fuel Sci. Technol*., 1987, **5**, 77-88.
41. V. Otero, D. Sanches, C. Montagner, M. Vilarigues, L. Carlyle, J.A. Lopes and M.J. Melo, *J. Raman Spectrosc*., 2013, **45**, 1197-1206.
42. K.L. Orchard, J.E. Harris, A.J.P. White, M.S.P. Shaffer and C.K. Williams, *Organometallics,* 2011*,* **30**, 2223-2229.
43. K.L. Orchard, M.S.P. Shaffer and C.K. Williams, *Chem. Mater*., 2012, **24**, 2443-2448.
44. K. L. Orchard, A.J.P. White, M.S.P. Shaffer and C.K. Williams, *Organometallics*, 2009, **28**, 5828-2832.
45. B. Vidjayacoumar, D.J.H. Emslie, J.M. Blackwell, S.B. Clendenning and J.F. Britten, *Chem. Mater*., 2010, **22**, 4844-4853.
46. V. Vishwanathan, K.-W. Jun, J.-W. Kim and H.-S. Roh, *Appl. Catal. A,* 2004, **276**, 251-255.
47. X.D. Peng, B.A. Toseland and R.P. Underwood, *Stud. Surf. Sci. Catal*., 1997, 175-182
48. A. Garcia-Trenco, A. Vidal-Moya and A. Martínez, *Catal. Today*, 2012, **179**, 43-51
49. T. Fujitani and J. Nakamura, *Appl. Catal. A,* 2000, **191**, 111-129
50. C.V. Ovesen, B.S. Clausen, J. Schiøtz, P. Stoltze, H. Topsøe, J.K. Nørskov, *J. Catal.,* 1997, **168**, 133-142.
51. J. Yoshihara and C.T. Campbell, *J. Catal.,* 1996*,* **161**, 776-782.
52. M. Behrens, F. Studt, I. Kasatkin, S. Kühl, M. Hävecker, F. Abild-Pedersen, S. Zander, F. Girgsdies, P. Kurr, B.-L. Kniep, M. Tovar, R. W. Fischer, J.K. Nørskov and R. Schlögl, *Science,* 2012, **336**, 893-897.
53. C. Tisseraud, C. Comminges, T. Belin, H. Ahouari, A. Soualah, Y. Pouilloux and A. Le Valant, *J. Catal*., 2015, DOI: 10.1016/j.jcat.2015.04.035
54. A. García-Trenco and A. Martínez, *Catal. Today,* 2014, **227**, 144-153.
55. D. Song, W. Cho, D.K. Park and E.S. Yoon, *J. Ind. Eng. Chem*., 2007, **13**, 815-826.
56. M.S. Spencer, *Top. Catal*., 1999, **8**, 259-266.

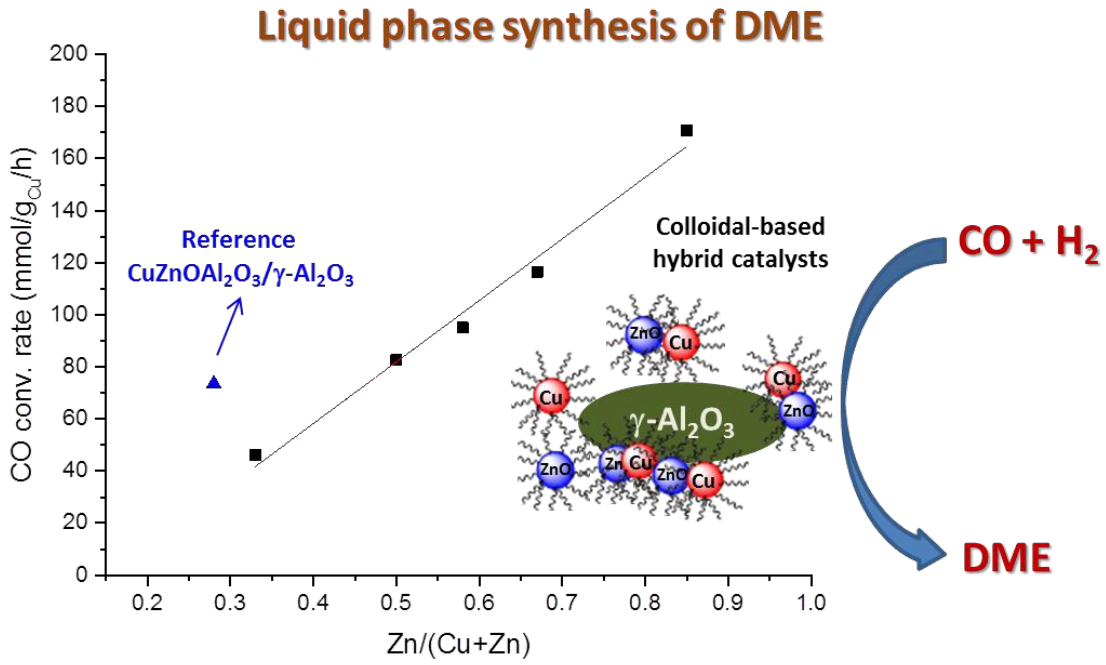

Colloidal Cu/ZnO nanoparticles combine with γ-Al_2O_3 to form promising hybrid catalysts for the direct synthesis of dimethyl ether (DME) in liquid phase, showing high activity, selectivity and stability.